J. Astrophys. Astr. (2010) **31,** 165–175

Solar Cycle Variation of Interplanetary Coronal Mass Ejection Latitudes

P. X. Gao[1,2,*] & K. J. Li[1,3]
[1]*National Astronomical Observatories/Yunnan Observatory, Chinese Academy of Sciences, Kunming 650 011, China.*
[2]*Graduate University of Chinese Academy of Sciences, Beijing 100 049, China.*
[3]*Key Laboratory of Solar Activity, National Astronomical Observatories, Chinese Academy of Sciences, Beijing 100 012, China.*
[*]*email: gaopengxin@ynao.ac.cn*

Received 2009 October 12; Accepted 2010 August 25

Abstract. With the use of interplanetary coronal mass ejections (ICMEs) compiled by Richardson and Cane from 1996 to 2007 and the associated coronal mass ejections (CMEs) observed by the Large Angle and Spectrometric Coronagraph (LASCO) onboard the Solar and Heliospheric Observatory (SOHO), we investigate the solar cycle variation of real ICME-associated CME latitudes during solar cycle 23 using Song *et al.*'s method. The results show the following:

- Although most of ICME-associated CMEs are distributed at low latitudes, there is a significant fraction of ICME-associated CMEs occurring at high latitudes.
- The latitudinal evolution of ICME-associated CMEs do not follow Spörer's sunspot law at low latitudes (thus, no 'butterfly diagram'); however, at high latitudes, there may be a poleward motion and an equatorward motion from the rise to the maximum to the declining phases.

Key words. Sun: activity, coronal mass ejections (CMEs).

1. Introduction

Interplanetary coronal mass ejections (ICMEs), i.e., the interplanetary manifestations of coronal mass ejections (CMEs), are responsible for the severest of geomagnetic storms when they impinge upon Earth's magnetosphere. In fact, Earth spends in the flows related to ICMEs anywhere from 10% of the time during solar minimum to 35% of the time during solar maximum (Richardson *et al.* 2002; Cliver *et al.* 2003). Thus, studies on ICMEs are important because of their direct connection to space environment.

Webb *et al.* (2000) showed that halo CMEs associated with surface activity within $0.5R_{\odot}$ of Sun center appear to be an excellent indicator of increased geoactivity several days later. Then, it is found that the solar sources of those CMEs that intercepted Earth mainly located within latitude $\pm 30^{\circ}$ (Gopalswamy 2002; Wang *et al.* 2002;

Reinard 2005). Recently, Riley *et al.* (2006) showed the evolution of the source latitude of halo CMEs for which a corresponding ICME could be identified in 1 AU inecliptic data. They found that the solar sources of halo CMEs with ICME counterpart followed the butterfly diagram. A similar conclusion was drawn by Gopalswamy (2006) and Gopalswamy *et al.* (2010). Gopalswamy *et al.* (2008), who separated magnetic clouds (MCs) from non-cloud (NC) ICMEs, also found that the solar sources of MCs followed the butterfly diagram.

However, Wang *et al.* (2002) identified 132 earth-directed halo CMEs and showed the location distributions of geoeffective halo CMEs and all the frontside halo CMEs. They found that, for geoeffective halo CMEs, the majority of these CMEs (81%) occurred within latitude $\pm(10^\circ$–$30^\circ)$ and only two events (3%) within the total 59 geoeffective halo CMEs were out of the latitude $\pm 40^\circ$; for all the frontside halo CMEs, they also were mainly ($\sim$78%) located within latitude $\pm(10^\circ$–$30^\circ)$ and only 8% frontside halo CMEs erupting outside of the latitude $\pm 40^\circ$. That is to say, there is no difference between the latitudinal distributions of geoeffective halo CMEs and all the frontside halo CMEs from the statistical point of view. Later, Riley *et al.* (2006) compared the evolution of the source latitude of halo CMEs for which a corresponding ICME could be identified in 1 AU inecliptic data and those for which one could not and found that there appeared to be no systematic difference between the source latitude of halo CMEs that intercepted Earth, and those that did not.

It must be pointed out that the aforementioned source latitude of CMEs was identified with the heliographic latitude of the associated surface event, such as flare, filament eruption and so on, or the associated activity, which is seen in EUV or soft X-rays. Howard *et al.* (2008) also identified solar surface source regions of CMEs using X-ray and Hα flare and disappearing filament data. They obtained the longitude from the associated flare or disappearing filament. However, for each CME measurement, the central position angle (CPA) was converted to solar latitude, which was used in preference to the latitude of the surface flare event (Howard *et al.* 2008). First, there is not a one-to-one correspondence between CME and flare location as flares are localized at a particular region of the Sun while CMEs often span several 10's of degrees of solar latitude. Flares also have a tendency to occur at one footpoint of the CME, as suggested by the difference in trends between Fig. 2(b) and 2(c) of Howard *et al.* (2008). Therefore, the associated flare may not be a true indicator of the 'central latitude' of the whole CME structure (Howard *et al.* 2008). There is no clear evidence of a direct link between the (hot) material seen in EUV and/or soft X-rays and the CME material seen in white light (Lara 2008).

Gopalswamy *et al.* (2003) converted the observed CPA of the prominent events and CME events to heliographic latitudes by assuming that the events happen in the plane of the sky and established that prominent eruptions and CMEs are closely related and had similar latitude dependence. A similar conclusion was drawn by Hundhausen (1993). Nevertheless, recently, Li *et al.* (2008) showed the latitude distributions of high-latitude (with their unsigned latitudes higher than 50°) and low-latitude (with their unsigned latitudes lower than 50°) filaments and found that there is an equatorward migration at low latitudes and a poleward migration at high latitudes; Li *et al.* (2009) showed the latitude distributions of high-latitude and low-latitude CMEs and found that there is no equatorward drift at low latitudes and no poleward drift at high latitudes. As we know, the usage of apparent latitude comes from the observed CPA of CME events

may also introduce a source of error. With the assumption that CMEs move radially, their longitudinal distribution is uniform, and they are all detected, Skirgiello (2003) proposed a mathematical tool using the apparent latitude distribution to deduce the real latitude distribution. By referring to this idea, Song *et al.* (2007) designed a much simpler and easier new method with the same function in order to obtain the evolution of real CME latitudes. Then, they investigated the evolution of real CME latitudes and found that the latitudinal evolution of low-latitude CMEs did not follow Spörer's sunspot law. However, they found that, at high latitudes, there is a poleward motion and an equatorward motion primarily during the years 1999–2001. Thus, although filaments often have extended sizes/lengths on the solar disc, the central latitude of filament may also not be a true indicator of the 'central latitude' of the whole CME structure.

According to the aforementioned results, we can find that the latitude of the associated surface event or activity might not represent the source latitude of CMEs. And the projection effect has very considerable influence on the latitude distribution of CMEs. Thus, it is necessary to determine whether ICME-associated CMEs originate from low latitude source magnetic structures and their sources follow the sunspot butterfly diagram applied the mathematical tool using the apparent latitude distribution to deduce the real latitude distribution. In this study, using the method of Song *et al.* (2007), we investigate the solar cycle variation of the real ICME-associated CME latitudes during solar cycle 23. This study will help us to understand whether the CME latitude is an important indicator for forecasting CME with ICME counterpart.

2. Method

Based on the assumption of radial motion and uniform longitudinal distribution of CMEs, Song *et al.* (2007) obtained a transformation matrix, M, from the apparent latitude distribution to the real latitude distribution. In other words, they arrived at

$$R = M^{-1} \times S, \tag{1}$$

where M is a 91×91 matrix (see section 3 of Song *et al.* 2007 for details). S is the distribution of the apparent latitude δ,

$$S = (s_0, s_1, \ldots, s_i, \ldots, s_{90})^T, \tag{2}$$

s_i means the percentage at $\delta = i^\circ$. In their study, S is smoothed with a window of 10°. R is the distribution of the real latitude θ,

$$R = (r_0, r_1, \ldots, r_i, \ldots, r_{90})^T, \tag{3}$$

r_i means the percentage at $\theta = i^\circ$. The final results of R also is smoothed with a window of 10° in their study.

In the present work, we compute the probability of ICME-associated CMEs corresponding to $\delta = 0^\circ, 1^\circ, \ldots, 90^\circ$. That is to say, s_i means the probability at $\delta = i^\circ$. Thus, based on the transformation matrix M, we can obtain r_i that means the probability at $\theta = i^\circ$. S and R are also smoothed with a window of 10°.

3. Solar cycle variation of ICME-associated CME latitudes

The ICME data used here were obtained from an ongoing study described by Cane and Richardson (2003). They represented the best estimate of ICMEs in the near-earth solar wind during this period, based on data from all available spacecraft and using a broad range of ICME signatures to identify events (Riley *et al.* 2006). When possible they also identified the source CME. On May 16, 2008, they have updated their list to include data up to 2007 and we use their new event list (with 307 events) for this analysis (Richardson and Cane 2008; henceforth RC2008). From the RC2008 event list, we select 130 events which were well associated with a single source CME. The associated CME data used here come from the Large Angle and Spectrometric Coronagraph onboard the Solar and Heliographic Observatory (SOHO/LASCO), available at http://cdaw.gsfc.nasa.gov/CME_list/.

In order to study the apparent latitude distribution of ICME-associated CMEs, we convert CPAs or measurement position angles (MPAs) to projected heliographic latitudes. For example, CPAs or MPAs of 0°, 90°, 180°, and 270° correspond to the apparent latitudes of 90°, 0°, -90°, and 0°, respectively. The CPA, which is in accordance with the CMEs whose spans were less than 360°, was defined as the mid angle with respect to the two edges of the CME in the sky plane. The MPA, which is in connection with the halo CMEs whose spans were 360°, is the angle between the line along the Solar North and the line connecting the CME's fastest leading edge and the solar disc center. Ideally, the MPA and CPA must be the same. However, some CMEs move nonradially so the two do not coincide.

Figure 1 shows the apparent latitudes of ICME-associated CMEs varying with time during solar cycle 23. From Fig. 1, we can find that, consistent with studies on the general population of CMEs (Hundhausen 1993; Li *et al.* 2009), ICME-associated CMEs are distributed over almost all apparent latitudes and there is no equatorward drift at low apparent latitudes (thus, no 'butterfly diagram') and no poleward drift at high apparent latitudes.

Then we compute the probability of ICME-associated CMEs correspond to $\delta = 0^\circ, 1^\circ, \ldots, 90^\circ$ during solar cycle 23. And, based on the transformation matrix M

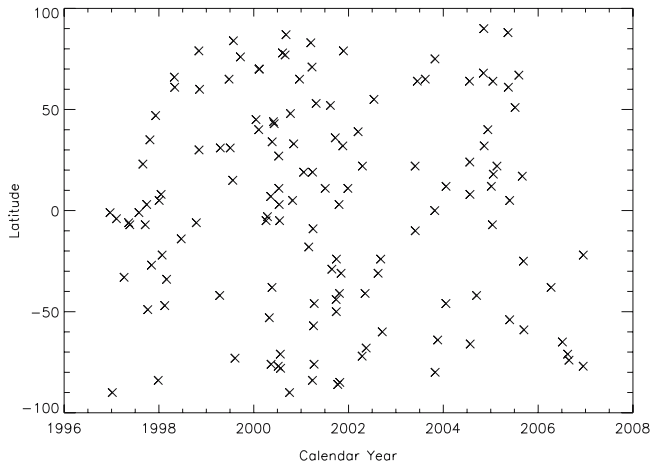

Figure 1. The apparent latitudes of ICME-associated CMEs changing with time during solar cycle 23.

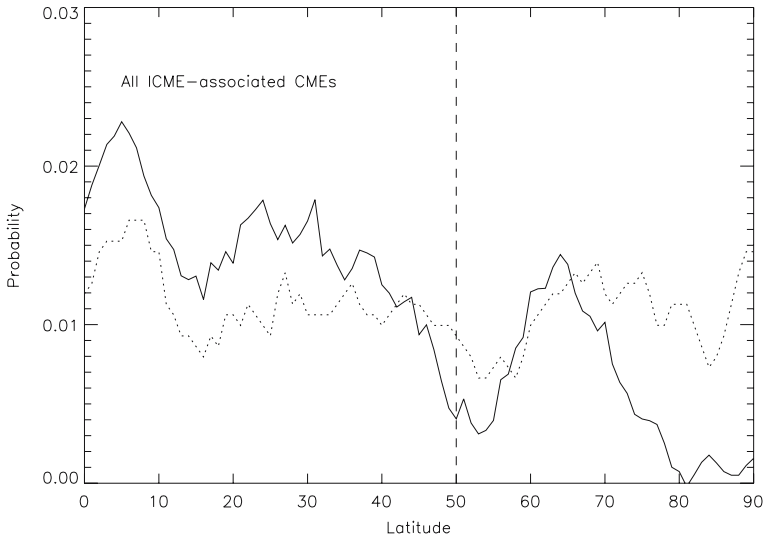

Figure 2. Distributions of the apparent (dotted line) and real (solid line) ICME-associated CME latitudes during solar cycle 23 that are smoothed with a window of 10°. The vertical dashed line represents latitude = 50°.

obtained by Song *et al.* (2007), we can obtain the probability of ICME-associated CMEs correspond to $\theta = 0°, 1°, \ldots, 90°$ during solar cycle 23. Distributions of the apparent and real ICME-associated CME latitudes are smoothed with a window of 10° in Fig. 2. It is found that there is a significant fraction of ICME-associated high apparent latitude CMEs are substituted with events coming from low latitudes, consistent with studies on the general population of CMEs (Song *et al.* 2007). Before the correction, there are 81 (59.1%) low apparent latitude ICME-associated CMEs and 56 (40.9%) high apparent latitude ICME-associated CMEs. In this study, S (the distribution of the apparent latitude δ) in equation (1) is smoothed with a window of 10°. So, we can only estimate the numbers of high latitude ICME-associated CMEs. From Fig. 2, we find that, after the correction, 76.5% of all the ICME-associated CMEs (about 105 ICME-associated CMEs) are distributed at low latitudes (0°–50°) and 23.5% of all the ICME-associated CMEs (about 32 ICME-associated CMEs) are distributed at high latitudes (51°–90°) during solar cycle 23. From Figs. 1 and 4(a) of Song *et al.* (2007), we also find that, during almost an entire solar cycle 23 (1996–2006), although most of CMEs are distributed at low latitudes, there is a significant fraction of CMEs occurring at high latitudes. That is to say, our results about the ICME-associated CME latitude distribution are consistent with studies on the general population of CMEs (Song *et al.* 2007).

To be sure that the difference seen between apparent and real latitude distributions of ICME-associated CMEs is not an effect of north-south asymmetry, we also compute the probability of the occurrence of ICME-associated CMEs with particular apparent and real latitude separately for the northern and southern hemispheres. Distributions of the apparent and real ICME-associated CME latitudes separately for the northern and southern hemispheres are also smoothed with a window of 10° in Fig. 3. The apparent and real ICME-associated CME latitude distributions separately for the northern and southern hemispheres have a slight difference. However, it is also found

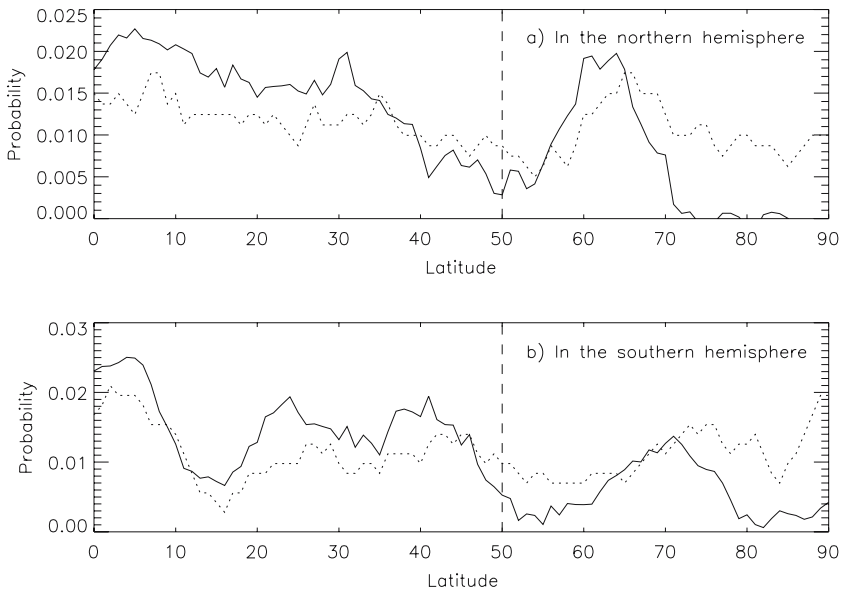

Figure 3. Distributions of the apparent (dotted line) and real (solid line) ICME-associated CME latitudes during solar cycle 23 separately for the northern **(a)** and southern **(b)** hemispheres that are smoothed with a window of 10°. The vertical dashed lines represent latitude = 50°.

that, in both the northern and southern hemispheres, there is a significant fraction of ICME-associated high apparent latitude CMEs that are substituted with events coming from low latitudes. Before the correction, in the northern hemisphere, there are 43 (58.9%) low apparent latitude ICME-associated CMEs and 30 (41.1%) high apparent latitude ICME-associated CMEs; in the southern hemisphere, there are 38 (59.4%) low apparent latitude ICME-associated CMEs and 26 (40.6%) high apparent latitude ICME-associated CMEs. From Fig. 3, we also find that, after the correction, there is a significant fraction of ICME-associated CMEs (24.1%, about 18 ICME-associated CMEs, in the northern hemisphere and 22.8%, about15 ICME-associated CMEs, in the southern hemisphere) occurring at high latitudes. In other words, the difference between apparent and real latitude distributions of ICME-associated CMEs is not an effect of north-south asymmetry.

In order to study the solar cycle variation of real ICME-associated CME latitudes, we divide the whole interval into 3 parts and investigate the real ICME-associated CME latitude distributions for each part, as shown in Fig. 4. That is to say, the real ICME-associated CME latitude distributions are shown grouped into three phases of the solar activity cycle: the rise phase (1996–1998), the maximum phase (1999–2002) and the declining phase (2003–2007). Distributions of the apparent and real ICME-associated CME latitudes during the three phases of cycle 23 are also smoothed with a window of 10°. Before the correction, there are 25 (71.4%) low apparent latitude ICME-associated CMEs and 10 (28.6%) high apparent latitude ICME-associated CMEs during the rise phase; there are 37 (58.7%) low apparent latitude ICME-associated CMEs and 26 (41.3%) high apparent latitude ICME-associated CMEs during the maximum phase and there are 19 (48.7%) low apparent latitude ICME-associated CMEs and 20 (51.3%) high apparent latitude ICME-associated CMEs during the declining phase. From Fig. 4,

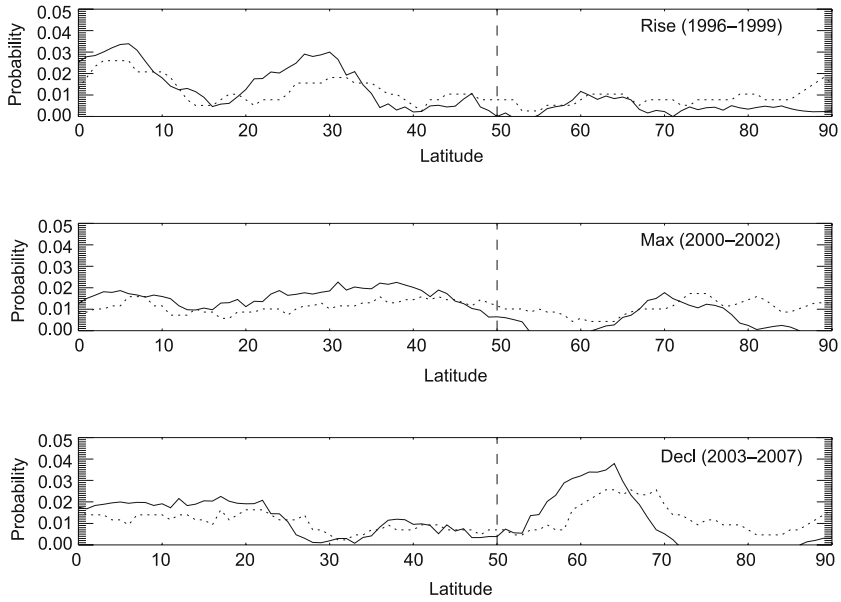

Figure 4. Distributions of the apparent (dotted line) and real (solid line) ICME-associated CME latitudes during the three phases of cycle 23 that are smoothed with a window of 10°. The vertical dashed lines represent latitude = 50°.

we can find that, after the correction, at low latitudes (0°–50°), the latitudinal evolution of ICME-associated CMEs does not follow the Spörer's sunspot law from the rise to the maximum to the declining phases. It is consistent with studies on the general population of CMEs (Song *et al.* 2007). For high latitude (50°–90°) ICME-associated CMEs, the majority of these CMEs (66%, or about 4 ICME-associated CMEs of all the about 6 ICME-associated CMEs) occur within latitude 55°–70° during the rise phase; the majority of these CMEs (89%, or about 11 ICME-associated CMEs of all the about 13 ICME-associated CMEs) occur within latitude 62°–82° during the maximum phase; the majority of these CMEs (97%, or about 15 ICME-associated CMEs of all the about 16 ICME-associated CMEs) occur within latitude 50°–70° during the declining phase. Our results seem to suggest that there may be a poleward motion and an equatorward motion at high latitudes from the rise to the maximum to the declining phases.

Then we also compute the probability of the occurrence of ICME-associated CMEs with particular apparent and real latitude during the three phases of cycle 23 separately for the northern and southern hemispheres. Distributions of the apparent and real ICME-associated CME latitudes during the three phases of cycle 23 separately for the northern and southern hemispheres are also smoothed with a window of 10° in Fig. 5. During the three phases of cycle 23, the apparent and real ICME-associated CME latitude distributions separately for the northern and southern hemispheres have a slight difference.

Before the correction, during the rise phase, there are 10 (58.8%) low apparent latitude ICME-associated CMEs and 7 (41.2%) high apparent latitude ICME-associated CMEs in the northern hemisphere and there are 15 (83.3%) low apparent latitude ICME-associated CMEs and 3 (16.7%) high apparent latitude ICME-associated CMEs in the southern hemisphere. During the maximum phase, there are 21 (63.6%)

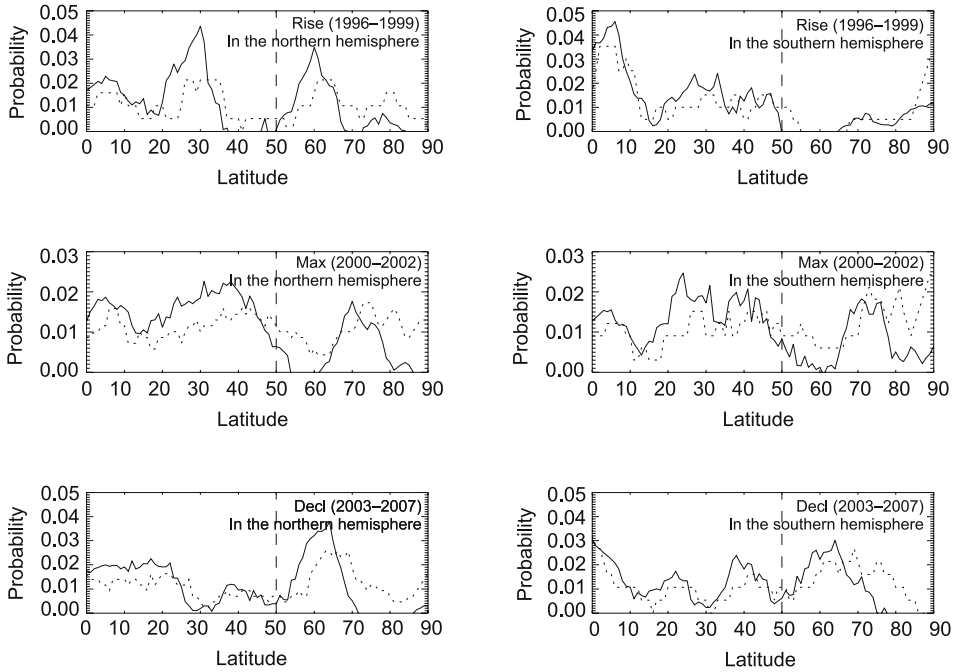

Figure 5. Distributions of the apparent (dotted line) and real (solid line) ICME-associated CME latitudes during the three phases of cycle 23 separately for the northern (left panel) and southern (right panel) hemispheres that are smoothed with a window of 10°. The vertical dashed lines represent latitude = 50°.

low apparent latitude ICME-associated CMEs and 12 (36.4%) high apparent latitude ICME-associated CMEs in the northern hemisphere and there are 16 (53.3%) low apparent latitude ICME-associated CMEs and 14 (46.7%) high apparent latitude ICME-associated CMEs in the southern hemisphere. During the declining phase, there are 12 (52.2%) low apparent latitude ICME-associated CMEs and 11 (47.8%) high apparent latitude ICME-associated CMEs in the northern hemisphere and there are 7 (43.8%) low apparent latitude ICME-associated CMEs and 9 (56.2%) high apparent latitude ICME-associated CMEs in the southern hemisphere.

From Fig. 5, we can find that, after the correction, at low latitudes, the latitudinal evolution of ICME-associated CMEs does not follow Spörer's sunspot law from the rise to the maximum to the declining phases in both the northern and southern hemispheres. For high latitude ICME-associated CMEs, in the northern hemisphere, the majority of these CMEs (88.1%, or about 5 ICME-associated CMEs of all the about 6 ICME-associated CMEs) occur within latitude 50°–70° during the rise phase; the majority of these CMEs (88.3%, or about 4 ICME-associated CMEs of all the about 5 ICME-associated CMEs) occur within latitude 61°–81° during the maximum phase; the majority of these CMEs (98.1%, or about 9 ICME-associated CMEs of all the about 10 ICME-associated CMEs) occur within latitude 50°–70° during the declining phase. That is, there may be a poleward motion and an equatorward motion from the rise to the maximum to the declining phases at high latitudes in the northern hemisphere.

However, for high latitude ICME-associated CMEs, in the southern hemisphere, the majority of these CMEs (91.5%, or about 2 ICMEs-associated CMEs of all the about

3 ICME-associated CMEs) occur within latitude 70°–90° during the rise phase; the majority of these CMEs (80.5%, or about 8 ICMEs-associated CMEs of all the about 9 ICME-associated CMEs) occur within latitude 65°–85° during the maximum phase; the majority of these CMEs (91.3%, or about 6 ICME-associated CMEs of all the about 7 ICME-associated CMEs) occur within latitude 50°–70° during the declining phase. In the southern hemisphere, there is no poleward motion, but there is an equatorward motion at high latitudes. That is to say, in the southern hemisphere, the latitudinal evolution of high latitude ICME-associated CMEs is different from those in the northern hemisphere and on the full solar disk. The reason might be that, before the correction, there is the least high apparent latitude ICME-associated CME number (only 3 events) in the southern hemisphere during the rise phase and the number is too small to be able to represent the apparent latitude distribution. Thus, based on the transformation matrix M, we obtain the latitude distribution that cannot represent the real latitude distribution in the southern hemisphere during the rise phase.

4. Conclusions and discussion

We investigate the solar cycle variation of real ICME-associated CME latitudes during solar cycle 23 with the method of Song *et al.* (2007) by using the ICMEs compiled by Richardson and Cane (2008) from 1996 to 2007 and the associated CMEs observed by SOHO/LASCO. The results show the following:

- Although most of ICME-associated CMEs are distributed at low latitudes, there is a significant fraction of ICME-associated CMEs occurring at high latitudes.
- The latitudinal evolution of ICME-associated CMEs does not follow Spörer's sunspot law at low latitudes (thus, no 'butterfly diagram'); however, at high latitudes, there may be a poleward motion and an equatorward motion from the rise to the maximum to the declining phases.

The solar cycle variation of apparent CME latitudes was extensively studied in the past (Hundhausen 1993; St. Cyr *et al.* 2000; Gopalswamy *et al.* 2003; Yashiro *et al.* 2004; Li *et al.* 2009) and found that CMEs are distributed over almost all latitudes and there is no equatorward drift at low latitudes (thus, no 'butterfly diagram') and no poleward drift at high latitudes. However, the aforementioned apparent latitude of the CMEs are subject to the projection effect. Recently, some methods were designed in order to obtain the evolution of real CME latitudes (Skirgiello 2003; Song *et al.* 2007; Lara 2008). It is found that there is a significant fraction of CMEs occurring at high latitudes although most of CMEs are distributed at low latitudes; the latitudinal evolution of low-latitude CMEs did not follow Spörer's sunspot law and there is a poleward motion and an equatorward motion at high latitudes primarily during the years 1999–2001 (Song *et al.* 2007).

The statistical characteristics of the distribution and solar cycle variation of CME latitudes are different from those of sunspot groups. Nearly all the sunspot groups occur at low latitudes and solar cycle variation of sunspot group latitudes follow Spörer's sunspot law ('butterfly diagram'). We know that sunspots seem to be specified on active regions (AR), but CMEs are a kind of large-scale solar activity. Zhou *et al.* (2006) speculated that the associated solar surface activity of a CME may act as either triggers of instability of the globally-coupled magnetic flux systems with different spacial scales, or the local manifestation of the instability, while the real basis for

deciding CME properties should be the pre-CME large-scale source structures. Many reports (Gao *et al.* 2007; Peng and Hu 2007; Wang *et al.* 2007; Gao and Li 2008; Li *et al.* 2009) furnish evidences to support that CMEs are intrinsically associated with the source magnetic structure on a large spatial scale (Wang *et al.* 2006; Zhou *et al.* 2006). Thus, CMEs are intrinsically associated with the source magnetic structure on a large spatial scale (Wang *et al.* 2006; Zhou *et al.* 2006), and this may be the reason why the statistical characteristics of the distribution and solar cycle variation of CME latitudes are different from those of sunspot groups.

It is believed that the solar sources of those CMEs that intercepted Earth mainly located within latitude $\pm 30^{\circ}$ (Gopalswamy 2002; Wang *et al.* 2002; Reinard 2005). Recently, through investigating the solar sources of CMEs that intercepted Earth, some authors (Gopalswamy 2006; Riley *et al.* 2006; Gopalswamy *et al.* 2008, 2010) found that the solar sources of those CMEs followed the butterfly diagram. We find that there is a significant fraction of ICME-associated CMEs occurring at high latitudes although most of ICME-associated CMEs are distributed at low latitudes; the latitudinal evolution of ICME-associated CMEs does not follow Spörer's sunspot law at low latitudes (thus, no 'butterfly diagram') and, at high latitudes, there may be a poleward motion and an equatorward motion from the rise to the maximum to the declining phases. Our results are different from the aforementioned results. This results suggest that not all of ICME-associated CMEs originate from low latitude source magnetic structures and not all of their sources follow the sunspot butterfly diagram.

To some extent, our results about the solar cycle variation of real ICME-associated CME latitudes are consistent with those studied on the general population of CMEs. But, the period of the poleward motion and equatorward motion of high latitude ICME-associated CMEs is different from that of the general population of CMEs. We investigate the evolution of real ICME-associated CME latitudes and found that there is a poleward and an equatorward motions from the rise to the maximum to the declining phases; Song *et al.* (2007) investigated the evolution of general population of CME latitudes and found that there is a poleward and an equatorward motions occurred primarily during the years 1999–2001. From Figs. 1 and 4(a) of Song *et al.* (2007), most of high latitude CMEs occurred during the years 1999–2001 and the poleward and equatorward motions occurred primarily during this period. But, a few high latitude CMEs occurred during the rise and declining phases. The discrepancy should suggest that, in order to effectively predict whether a CME will encounter the Earth, other characteristics of CMEs should be taken into account.

In conclusion, our results seem to suggest that the interplanetary characteristics of CMEs and the characteristics of the source magnetic structures on a large spatial scale of the ICME-associated CMEs, such as longitudes of CMEs, the sign of magnetic helicity, the orientation of the source magnetic field and so on, should be taken into account in order to effectively predict whether a CME will encounter the Earth; however, the CME latitude should not be an important indicator for forecasting CME geoeffectiveness. Admittedly, the results of this study based on a relatively small number (137) of ICME-associated CMEs are far from complete and it requires further research.

Acknowledgements

We thank the anonymous referee for constructive comments that improved the original version. The CME catalogue used in this study is generated and maintained at the

CDAW Data Center by NASA and the Catholic University of America in co-operation with the Naval Research Laboratory. SOHO is a project of international co-operation between ESA and NASA. The work is supported by the National Natural Science Foundation of China (NSFC) under Grants 10873032, 10921303, and 40636031, the National Key Research Science Foundation (2006CB806303), and the Chinese Academy of Sciences.

References

Cane, H. V., Richardson, I. G. 2003, *JGR*, **108**, 1156.
Cliver, E. W., Ling, A. G., Richardson, I. G. 2003, *ApJ*, **592**, 574.
Gao, P. X., Li, Q. X., Zhong, S. H. 2007, *J. Astrophys. Astr.*, **28**, 207.
Gao, P. X., Li, K. J. 2008, *Chin. J. Astron. Astrophys. (ChJAA)*, **8**, 146.
Gopalswamy, N. 2002, *COSPAR Colloq. Ser.*, **14**, 157.
Gopalswamy, N., Shimojo, M., Lu, W., Yashiro, S., Shibasaki, K., Howard, R. A. 2003, *ApJ*, **586**, 562.
Gopalswamy, N. 2006, *Space Sci. Rev.*, **124**, 145.
Gopalswamy, N., Akiyama, S., Yashiro, S., Michalek, G., Lepping, R. P. 2008, *J. Atmos. Sol.-Terr. Phys.*, **70**, 245.
Gopalswamy, N., Akiyama, S., Yashiro, S., Makela, P. 2010, In: *Magnetic Coupling between the Interior and Atmosphere of the Sun* (eds) Hasan, S. S., Rutten, R. J., Astrophysics and Space Science Proceedings, Springer-Berlin-Heidelberg, pp. 289.
Howard, T. A., Nandy, D., Koepke, A. C. 2008, *JGR*, **113**, A01104.
Hundhausen, A. J. 1993, *JGR*, **98**, 13,177.
Lara, A. 2008, *ApJ*, **688**, 647.
Li, K. J., Li, Q. X., Gao, P. X., Shi, X. J. 2008, *JGR*, **113**, A11108.
Li, K. J., Gao, P. X., Li, Q. X., Mu, J., Su, T. W. 2009, *Sol. Phys.*, **257**, 149.
Peng, Z., Hu, Y. Q. 2007, *ApJ*, **668**, 513.
Reinard, A. 2005, *ApJ*, **620**, 501.
Richardson, I. G., Cane, H. V., Cliver, E. W. 2002, *JGR*, **107**, 1187.
Richardson, I., Cane, H. 2008, Near-Earth Interplanetary Coronal Mass Ejections in 1996–2007, revised 2008 May 16, http://www.ssg.sr.unh.edu/mag/ace/ACElists/ICMEtable.html.
Riley, P., Schatzman, C., Cane, H. V., Richardson, I. G., Gopalswamy, N. 2006, *ApJ*, **647**, 648.
Skirgiello, M. 2003, *GRL*, **30**, 1995.
Song, W. B., Feng, X. S., Hu, Y. Q. 2007, *ApJ*, **667**, L101.
St. Cyr, O. C., Howard, R. A., Sheeley Jr., N. R., Plunkett, S. P., Michels, D. J., Paswaters, S. E., Koomen, M. J., Simnett, G. M., Thompson, B. J., Gurman, J. B., Schwenn, R., Webb, D. F., Hildner, E., Lamy, P. L. 2000, *JGR*, **105**, 18169.
Wang, Y. M., Ye, P. Z., Wang, S., Zhou, G. P., Wang, J. X. 2002, *JGR*, **107**, 1340.
Wang J. X., Zhou G. P., Wen Y. Y., Zhang, Y. Z., Wang, H. N., Deng, Y. Y., Zhang, J., Harra, L. K. 2006, *Chin. J. Astron. Astrophys. (ChJAA)*, **6**, 247.
Wang, J. X., Zhang, Y. Z., Zhou, G. P., Harra, L. K., Williams, D. R., Jiang, Y. C. 2007, *Sol. Phys.*, **244**, 75.
Webb, D. F., Cliver, E. W., Crooker, N. U., St. Cyr, O. C., Thompson, B. J. 2000, *JGR*, **105**, 7491.
Yashiro, S., Gopalswamy, N., Michalek, G., St. Cyr, O. C., Plunkett, S. P., Rich, N. B., Howard, R. A. 2004, *JGR*, **109**, A07105.
Zhou G. P., Wang, J. X., Zhang, J. 2006, *A&A*, **445**, 1133.